Pharmacological Characterization of the Allosteric Modulator Desformylflustrabromine and Its Interaction with $\alpha4\beta2$ Neuronal Nicotinic Acetylcholine Receptor Orthosteric Ligands

Maegan M. Weltzin and Marvin K. Schulte

Department of Chemistry and Biochemistry, University of Alaska, Fairbanks, Alaska

Received March 2, 2010; accepted May 28, 2010

ABSTRACT

Neuronal nicotinic acetylcholine receptors (nAChRs) are members of the Cys-loop superfamily of ligand-gated ion channels. nAChRs are involved in modulating nicotinic-based signal transmission in the central nervous system and are implicated in a range of disorders. Desformylflustrabromine (dFBr) is a positive allosteric modulator that potentiates $\alpha4\beta2$ nAChRs. It has been reported that dFBr is selective for the $\alpha4\beta2$ receptor relative to other common nAChR subtypes (*Neurosci Lett* **373:** 144–149, 2005). Coapplication of dFBr with acetylcholine (ACh) produces a bell-shaped dose–response curve with a peak potentiation of more than 265% (*Bioorg Med Chem Lett* **17:**4855–4860, 2007) at dFBr concentrations <10 μM and inhibition of responses at concentrations >10 μM. The potentiation and inhibition components of dFBr-modulated responses were examined by using two-electrode voltage clamp and human $\alpha4\beta2$ nAChRs expressed in *Xenopus laevis* oocytes. Currents to both partial and full agonists were potentiated by dFBr. Responses to low-efficacy agonists were potentiated significantly more than responses to high-efficacy agonists. Antagonist pIC_{50} values were unaffected by coapplication of dFBr. In addition to its potentiating effects, dFBr was able to induce current spikes when applied to desensitized receptors, suggestive of a shift in equilibrium from the desensitized to open conformation. In contrast to potentiation, inhibition of ACh responses by dFBr depends on membrane potential and is probably the result of open-channel block by dFBr and ACh. Our data indicate distinct mechanisms for the potentiation and inhibition components of dFBr action. dFBr could prove useful for therapeutic enhancement of responses at $\alpha4\beta2$-containing synapses.

Introduction

The central nervous system expression of neuronal nicotinic acetylcholine receptor (nAChR) subtypes are altered in many neurological disorders, including Alzheimer's disease (Court et al., 2001; Nordberg, 2001), autism (Martin-Ruiz et al., 2004; Lippiello, 2006), Parkinson's disease (Aubert et al., 1992), and schizophrenia (Woodruff-Pak and Gould, 2002; Friedman, 2004; Adams and Stevens, 2007). In Alzheimer's disease, multiple subtypes of nAChRs decline, producing a decrease in cholinergic tone (Court et al., 2001; Nordberg, 2001). Postmortem studies of autistic people have shown both decreases and increases in nAChR subtypes (Court et al., 2001; Nordberg, 2001; Martin-Ruiz et al., 2004; Lippiello,

2006). Increases in receptor populations should be amenable to remediation with antagonists, but treatment of disorders involving decreases in receptor number is more difficult. Treatment strategies aimed at increasing activity of cholinergic systems have focused on acetylcholinesterase inhibitors and partial agonists (Bourin et al., 2003; Corey-Bloom, 2003; Nicolson et al., 2006). Although agonists are potentially useful therapeutically, the rapid desensitization of nAChRs produced by chronic exposure to agonists limits their usefulness.

Positive allosteric modulators (PAMs) represent an alternative treatment strategy. Because PAMs typically enhance agonist responses without activating receptors, synaptic currents remain linked to endogenous neurotransmitter release. In disorders where differential changes in nAChR densities occur nonselective compounds may improve some symptoms while exacerbating others. The development of subtype-selective PAMs is an important step in developing therapeutic treatments for neurological disorders involving alterations in nicotinic tone.

ABBREVIATIONS: nAChR, neuronal nicotinic acetylcholine receptor; PAM, positive allosteric modulator; dFBr, desformylflustrabromine; DHβE, dihydro-β-erythroidine; ACh, acetylcholine; DMAB, *p*-dimethylaminobenzaldehyde; *V/I*, voltage versus current; PNU-120596, 1-(5-chloro-2,4-dimethoxyphenyl)-3-(5-methylisoxazol-3-yl)urea.

Desformylflustrabromine (dFBr) is a novel PAM that potentiates ACh-induced whole-cell responses of the α4β2 nAChR subtype by more than 265% (3 μM dFBr coapplied with 100 μM ACh). Previous studies have shown no apparent potentiation of other subtypes, including α7 and α3β4 (Sala et al., 2005; Kim et al., 2007). On α4β2 receptors, coapplication of increasing concentrations of dFBr with a fixed concentration of ACh produces a bell-shaped dose–response curve containing both stimulatory (<10 μM dFBr) and inhibitory components (>10 μM dFBr) (Kim et al., 2007). On α7 receptors only the inhibitory component is present. Previous studies using dFBr extracted from *Flustra foliacea* suggested potentiation may be a result of altered channel gating kinetics (Sala et al., 2005). At inhibitory concentrations of dFBr "rebound" or "hump currents" have been observed, suggesting dFBr inhibition may be attributable to open-channel block (Kim et al., 2007).

The current study aims to better understand the mechanisms of dFBr potentiation and inhibition. We investigated both the inhibitory and potentiating actions of dFBr by using a series of full agonists, partial agonists, and antagonists. Our data suggest that inhibition and potentiation are mediated by distinct mechanisms at different binding sites. Inhibition seems to be the result of channel block by both dFBr and the stimulating agonist. dFBr was determined to potentiate low-efficacy agonists more than high-efficacy agonists and was capable of recovering receptors from desensitization. This supports the hypothesis that dFBr inhibition is caused by open-channel block, whereas potentiation is caused by a change in the equilibrium between open and desensitized conformations.

Materials and Methods

Receptors and RNA. The cDNA for human α4 and β2 nAChR subunits was generously provided by Dr. Jon Lindstrom (University of Pennsylvania, Philadelphia, PA). This cDNA was inserted into a pcDNA3.1/Zeo (Invitrogen, Carlsbad, CA) mammalian expression vector to produce mRNA for receptor expression in *Xenopus laevis* oocytes. *X. laevis* frogs and frog food were purchased from Xenopus Express (Homosassa, FL). Ovarian lobes were surgically removed from Finquel-anesthetized *X. laevis* frogs and washed twice in Ca^{2+}-free Barth's buffer (82.5 mM NaCl, 2.5 mM KCl, 1 mM MgCl_2, 5 mM HEPES, pH 7.4) then gently shaken with 1.5 mg/ml collagenase (Sigma type II; Sigma-Aldrich, St. Louis, MO) for 20 min at 20 to 25°C. Stage V and VI oocytes were selected for microinjection (University of Alaska Fairbanks Institutional Animal Care and Use Committee 08-71). No more than four surgeries were conducted on each frog. A recovery period longer than 6 weeks was allowed between repeat surgeries on the same animal. Synthetic cRNA transcripts for human α4β2 were prepared by using the T7 mMESSAGE mMACHINE High Yield Capped RNA Transcription Kit (Ambion, Austin, TX). Oocytes were injected with a total of 50 nl of cRNA at a concentration of 300 ng/μl and incubated at 19°C for 24 to 72 h before their use in voltage-clamp experiments. At least two different batches of oocytes were used per experiment. dFBr·HCl was synthesized by Dr. Richard Glennon (Virginia Commonwealth University, Richmond, VA) (Kim et al., 2007) and dissolved in ND-96 buffer (96 mM NaCl, 2 mM KCl, 1.8 mM CaCl_2, 1 mM MgCl_2, 5 mM HEPES, pH 7.4) before use.

Two-Electrode Voltage Clamp. Recordings were performed by using an automated two-electrode voltage-clamp system incorporating an OC-725C oocyte clamp amplifier (Warner Instruments, Hamden, CT) coupled to a computerized data acquisition (Datapac 2000; RUN Technologies, Mission Viejo, CA) and autoinjection system

(Gilson Inc., Middleton, WI). Recording and current electrodes with resistance 1 to 4 MΩ were filled with 3 M KCl. Details of the chambers and methodology used for electrophysiological recordings have been described previously (Joshi et al., 2004). Oocytes were held in a vertical flow chamber of 200-μl volume, clamped at a holding potential of −60 mV, and perfused with ND-96 recording buffer at a rate of 20 ml/min. For voltage step experiments, the holding potential was varied from −100 to +20 mV. Test compounds (Sigma-Aldrich and Tocris Bioscience, Ellisville, MO) were dissolved in ND-96 buffer and injected into the chamber at a rate of 20 ml/min by using an autosampler injection system (Gilson Inc., Middleton, WI).

Electrophysiology Dose–Response Experiments. Dose–response curves for the full agonist [acetylcholine·Cl (Sigma-Aldrich)] and the partial agonists [(−)-nicotine (Riedel-de-Haën, Seelze, Germany), choline·Cl (Sigma-Aldrich), and cytisine (Sigma-Aldrich)] were evaluated at concentrations ranging from 0.01 to 300 μM for ACh, nicotine, and cytisine and 0.1 μM to 30 mM for choline. The effects of dFBr on agonist efficacies were determined by coexposure of varied concentrations of agonist with 1 μM dFBr.

The competitive antagonists [dihydro-β-erythroidine (DHβE)·HBr (Tocris Bioscience), DMAB-anabaseine·2HCl (Tocris Bioscience), and tropisetrone·HCl (Tocris Bioscience)] were evaluated for their ability to inhibit responses to 1 mM ACh at antagonist concentrations ranging from 0.001 to 100 μM. The effect of dFBr on antagonist inhibition was determined by coexposing receptors to antagonist, 1 mM ACh, and 1 μM dFBr.

To permit comparison of responses from different oocytes, individual responses to drug application were normalized to control responses elicited by using 1 mM ACh. Data were collected from at least four replicate experiments using oocytes obtained from at least two different frogs.

Exposure of dFBr Before Agonist Activation and During Agonist-Induced Desensitization. To study the effects of dFBr before agonist activation (pre-exposure) on α4β2 nAChR, 1 μM dFBr was bath-applied at a rate of 4 ml/min 30 s before application of agonist. After pre-exposure to dFBr, 1 mM ACh was applied at a 20 ml/min perfusion rate for 3 s. The slope of the rising phase of the response was determined from current data during the linear portion of the response before the peak current. Slopes for pre-exposure and coexposure experiments were compared by using these data, and *p* values were calculated based on the null hypothesis using an unpaired *t* test.

dFBr was also applied during the desensitization refractory phase of the agonist response. In these "post-exposure" experiments, saturating concentrations of agonists (1 mM ACh, 10 mM ACh, or 100 μM cytisine) were bath-applied at a rate of 4 ml/min before exposure to dFBr. dFBr (1 μM) was applied at a rate of 20 ml/min in repeated 3-s pulses once the agonist response entered the refractory desensitized phase of the response. Responses were normalized to currents obtained by using the appropriate ACh concentration in the absence of dFBr. The slope of the rising phase of the response was determined from current data during the linear portion of the response before the peak current. The agonist- and dFBr-induced currents were compared by using *p* values calculated based on the null hypothesis using an unpaired *t* test.

The effects of long-term exposure to 1 μM dFBr on activated receptors were also investigated. ACh (1 mM) or 100 μM cytisine were bath-applied at a rate of 4 ml/min. Eight milliliters of 1 μM dFBr with and without agonist was perfused at a rate of 10 ml/min for 48 s to desensitized receptors. As a control, 1 mM ACh was bath-applied, whereas 1 mM ACh was perfused for 48 s at the onset of the maximum induced response. Alterations in the response currents were examined.

Voltage Step Experiments. The voltage dependence of both dFBr potentiation and inhibition was determined by using α4β2-expressing *X. laevis* oocytes and two-electrode voltage clamp. The membrane potential was incrementally increased in 10-mV steps ranging from −100 to +20 mV. Cytisine was chosen as the stimu-

lating ligand for these experiments because it has been previously shown to not induce channel block of nAChRs at 100 μM (Liu et al., 2008). dFBr at either 10 μM (potentiating concentration) or 30 μM (inhibitory concentration) was coapplied with a fixed concentration of 100 μM cytisine (saturating concentration) at each voltage step. Responses were normalized to the response obtained at a membrane potential of −60 mV and 1 mM acetylcholine applied alone. The membrane potential (V_m) was plotted against the normalized current. The slope of the V_m versus I plot was determined by using linear regression.

Data Analysis. Concentration/response curves were fit by using nonlinear curve fitting and Prism Software (GraphPad Software, Inc., San Diego, CA) with standard built-in algorithms. Values for the log EC_{50} and n_H were determined by fitting the concentration response data to a single site binding model:

$$I = \frac{b + (I_{max} - b)}{1 + 10^{(logEC_{50} - [L])*n_H}} \quad (1)$$

where I is the current elicited on application of agonist, b is the baseline current in the absence of ligand, L is the ligand concentration, and n_H is the Hill slope. The EC_{50} value is the concentration of agonist producing currents equal to half of the maximal current (I_{max}). The pEC_{50} values reported reflect the negative log of the EC_{50}. EC_{50} values were also calculated from the $logEC_{50}$ and are included for convenience. I_{max} values for different partial and full agonists were compared with relative apparent efficacies and apparent efficacy changes as a result of dFBr coapplication. To permit comparison of full and partial agonist data from different oocytes, responses for all test compounds were normalized to the currents obtained with 1 mM ACh in the absence of dFBr.

For inhibition experiments, pIC_{50} ($-\log IC_{50}$) and IC_{50} values were determined by fitting concentration/response data to a single-site competition model:

$$I = \frac{b + (I_{max} - b)}{1 + 10^{([L] - logIC_{50})}} \quad (2)$$

where I is the current at a specific inhibitor/agonist concentrations, b is the baseline current in the absence of agonist, and L is the ligand concentration. The IC_{50} value is the concentration of antagonist that reduces the current to half that obtained by the identical concentration of agonist alone. The pIC_{50} values reported reflect the negative log of the IC_{50}. pIC_{50} values were typically determined at agonist concentrations equal to the EC_{50} for the agonist used. To compare data from different oocytes, currents were normalized to those obtained from application of 1 mM ACh alone. For experiments involving coperfusions of both an antagonist and agonist with dFBr, responses were normalized to those obtained by coperfusion of 1 μM dFBr with 1 mM ACh.

Comparisons of pEC_{50} or pIC_{50} values were conducted by using an unpaired t test, and p values were calculated based on the null hypothesis.
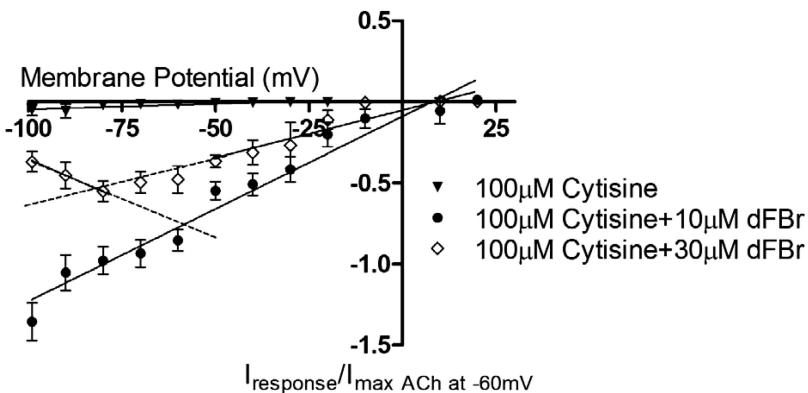
Results

dFBr Inhibition Involves Open-Channel Block. Understanding the nature of dFBr inhibition is essential to correctly interpreting overall response kinetics. Clues to the mechanism of dFBr inhibition come from previous studies of dFBr that show the presence of hump currents during washout of dFBr and agonist (Kim et al., 2007). Hump currents, also known as rebound currents, are inward currents that occur during the desensitized phase of the response on washout of the ligand. Hump currents have been previously linked to open-channel block (Liu et al., 2008) and are thought to be induced when an agonist binds with high affinity to the orthosteric site and lower affinity in the channel. During washout of the ligand, the ligand bound to the channel dissociates more rapidly, thus removing the channel block and producing transient increases in the observed response. The observation of hump currents suggests dFBr inhibition may involve channel block. To explore this possibility, we evaluated the inhibition of cytosine-induced currents at a series of different membrane potentials. Cytisine was chosen for these experiments because it is a known partial agonist that does not seem to act as a channel blocker (Liu et al., 2008) (Fig. 1). Although other more efficacious agonists could have been used for these experiments, the ability of these agonists to channel block would have complicated analysis of the results, making it difficult to determine whether any observed channel block is caused by the stimulating agonist or dFBr. Increased membrane potential will typically reduce channel block, thus increasing conductance at higher potentials as indicated by increased slopes in plots of voltage versus current (V/I). Figure 1 shows a V/I plot obtained by coapplication of dFBr with 100 μM cytisine at both potentiating and inhibiting dFBr concentrations. At concentrations of dFBr that are potentiating rather than inhibiting (10 μM) coexposure of 100 μM cytisine (saturating concentration of cytisine) produces a V/I plot that is linear over the entire range of membrane potentials tested. This verifies the lack of channel block by cytisine. In contrast, coapplication of a higher inhibitory concentration of dFBr (30 μM) with 100 μM cytisine produces a V/I plot that is nonlinear over the range of membrane potentials tested.

dFBr Potentiates Low Efficacious Agonists More Than Full Agonists. Partial agonists are useful tools in studying mechanisms of allosteric modulators. Changes in response profiles, I_{max}, and pEC_{50} values for partial agonists that result from the addition of a modulator, such as dFBr,

Fig. 1. Voltage dependence of potentiation and inhibition by dFBr. Membrane potential was increased in 10-mV steps from −100 to +20 mV using a two-electrode voltage clamp on α4β2 nAChR-expressing oocytes. Responses were obtained as discussed under *Materials and Methods* and normalized to those elicited by application of 1 mM ACh at −60 mV from the same oocyte. At least two batches of oocytes from different frogs were harvested for the experiments. Each data point represents at least $n \geq 4$ replicates with error bars shown as ± S.E.M. For the control group (100 μM cytisine) the relationship between the induced response and the applied membrane potential is linear over the entire range of membrane potentials. Potentiating concentrations of dFBr (10 μM) coapplied with 100 μM cytisine show a similar linear relationship. Coapplication of 30 μM dFBr (inhibitory concentration) with 100 μM cytisine shows a nonlinear relationship between membrane potential and the induced response.
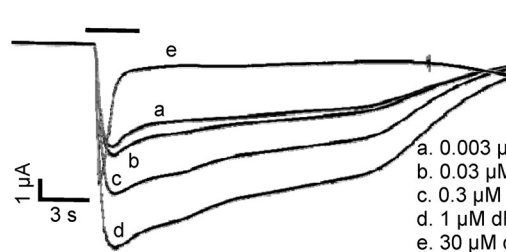
A ACh

ACh EC₅₀
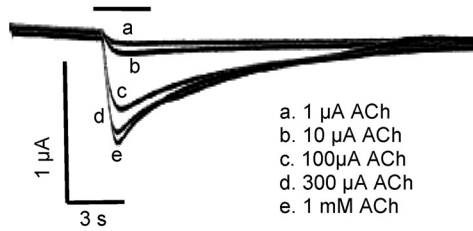
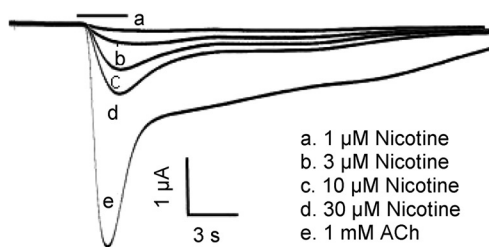a. 1 µA ACh
b. 10 µA ACh
c. 100µA ACh
d. 300 µA ACh
e. 1 mM ACh

dFBr + 100 µM ACh

a. 0.003 µM dFBr + 10 µM Nicotine
b. 0.03 µM dFBr + 10 µM Nicotine
c. 0.3 µM dFBr + 10 µM Nicotine
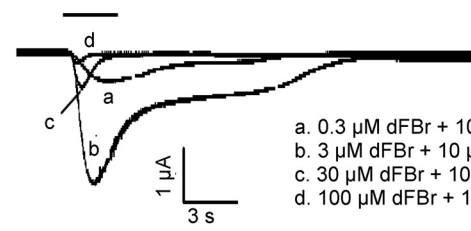d. 1 µM dFBr + 10 µM Nicotine
e. 30 µM dFBr + 10 µM Nicotine

B Nicotine

Nicotine EC₅₀

a. 1 µM Nicotine
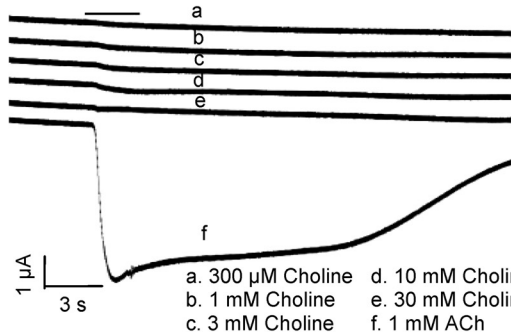b. 3 µM Nicotine
c. 10 µM Nicotine
d. 30 µM Nicotine
e. 1 mM ACh

dFBr + 10 µM Nicotine

a. 0.3 µM dFBr + 10 µM Nicotine
b. 3 µM dFBr + 10 µM Nicotine
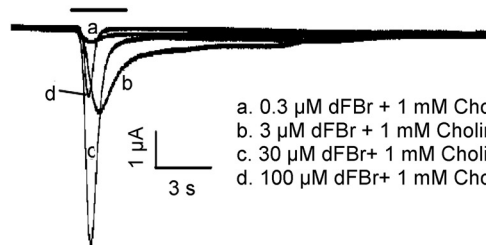c. 30 µM dFBr + 10 µM Nicotine
d. 100 µM dFBr + 10 µM Nicotine

C Choline

Choline EC₅₀

a. 300 µM Choline   d. 10 mM Choline
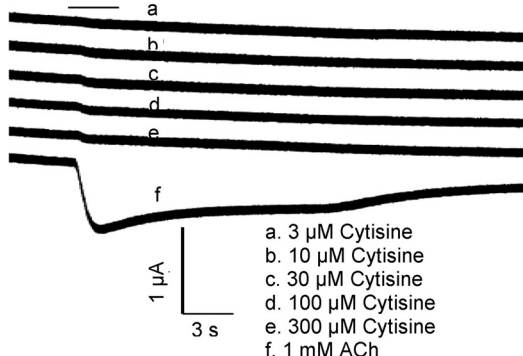b. 1 mM Choline   e. 30 mM Choline
c. 3 mM Choline   f. 1 mM ACh

dFBr + 1 mM Choline

a. 0.3 µM dFBr + 1 mM Choline
b. 3 µM dFBr + 1 mM Choline
c. 30 µM dFBr+ 1 mM Choline
d. 100 µM dFBr+ 1 mM Choline

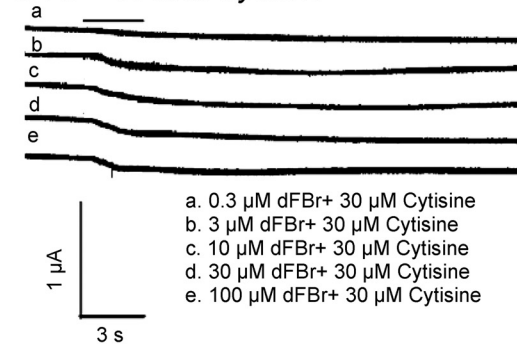## D Cytisine

Cytisine EC₅₀

a. 3 µM Cytisine
b. 10 µM Cytisine
c. 30 µM Cytisine
d. 100 µM Cytisine
e. 300 µM Cytisine
f. 1 mM ACh

dFBr + 30 mM Cytisine

a. 0.3 µM dFBr+ 30 µM Cytisine
b. 3 µM dFBr+ 30 µM Cytisine
c. 10 µM dFBr+ 30 µM Cytisine
d. 30 µM dFBr+ 30 µM Cytisine
e. 100 µM dFBr+ 30 µM Cytisine

Fig. 2. dFBr-modulated responses to nAChR agonists and partial agonists. Responses were obtained from *Xenopus* oocytes under voltage-clamp conditions ($V_m = -60$ mV). Left, responses to agonists alone. Right, traces obtained at increasing concentrations of dFBr coapplied with fixed concentrations of either acetylcholine (A), nicotine (B), choline (C), or cytisine (D). Shown are the concentrations of agonist applied alone (left) or the concentration of dFBr and coapplied (right). The solid bar above the response traces indicates the time the oocyte was exposed to the agonist and/or dFBr. All traces for each set of responses were recorded from a single oocyte expressing α4β2 receptors (mRNA injected at a ratio of 1α/1β). Similar data obtained at varied agonist concentrations were pooled, and the data were plotted to produce the dose–response curves shown in Fig. 3 and the data shown in Table 1.
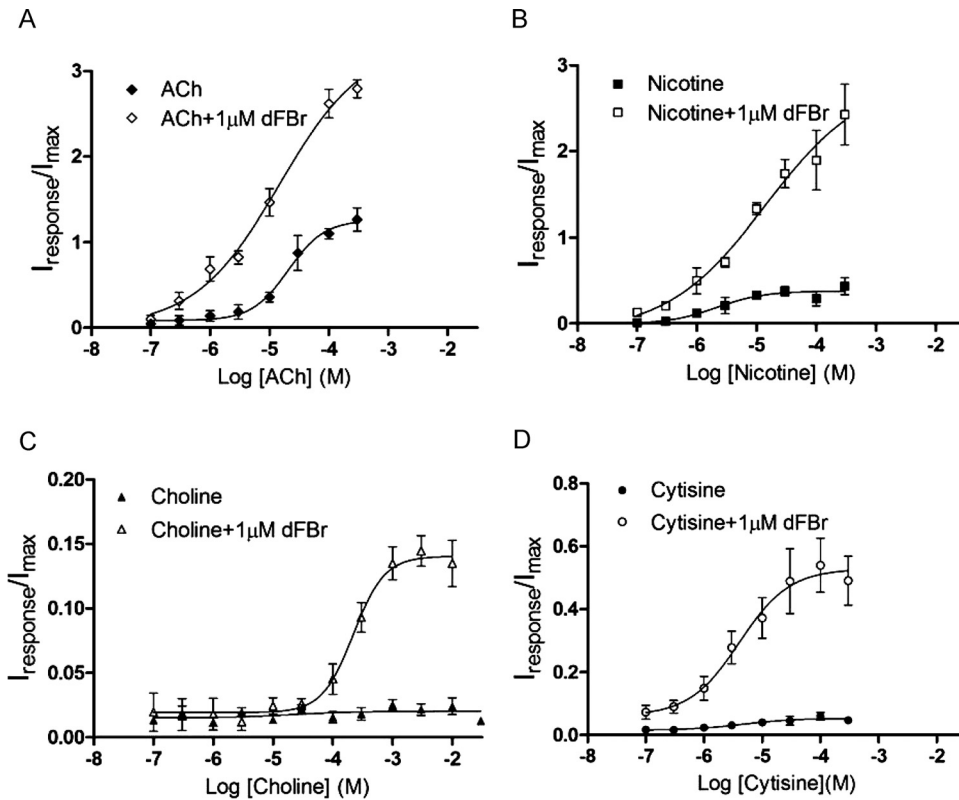
Fig. 3. Dose–response curves for agonists and partial agonists in the presence and absence of 1 μM dFBr. A, ACh. B, nicotine. C, choline. D, cytisine. dFBr and the appropriate concentration of agonist or partial agonist were coapplied to *Xenopus* oocytes expressing α4β2 receptors (mRNA injected at a ratio of 1α/1β). The peak current was measured, and responses were normalized to currents elicited by 1 mM ACh applied alone to the same oocyte. Each data point represents the combined data from at least four different experiments from a minimum of two different oocytes harvested from different frogs. Error bars indicate ± S.E.M. pEC_{50}, I_{max}, and Hill slope (n_H) were calculated by using nonlinear curve fitting algorithms and are shown in Table 1.

TABLE 1
dFBr induced effects on response kinetics for agonists and partial agonists

The data were obtained by using nonlinear curve fitting algorithms from the dose–response curves shown in Fig. 2. Because individual responses were normalized to the response elicited by 1 mM ACh alone, the I_{max} value shown represents the maximum current elicited relative to that obtained with 1 mM ACh in the absence of dFBr. Values in brackets indicate the fractional change in the value resulting from coapplication of 1 μM dFBr. The statistical significance of observed differences in pEC_{50}, I_{max}, and n_H as a result of 1 μM dFBr coapplication was evaluated by using a paired Student's *t* test. *P* values are given in parentheses under the fold change. Values were considered statistically different at $p \leq 0.0001$.

Ligand	$pEC_{50} \pm$ S.E.M. [EC_{50} (μM)]		$I_{max} \pm$ S.E.M.		$n_H \pm$ S.E.M.	
	0 μM dFBr	1 μM dFBr [Fold Change]	0 μM dFBr	1 μM dFBr [Fold Change]	0 μM dFBr	1 μM dFBr [Fold Change]
ACh	4.7 ± 0.1 (21)	4.8 ± 0.3 (15) [1.0] (P = 0.58)	1.3 ± 0.10	3.3 ± 0.6 [2.7] (P < 0.0001)	1.4 ± 0.5	0.6 ± 0.2 [0.43] (P = 0.21)
Nicotine	5.7 ± 0.3 (2.1)	4.9 ± 0.5 (14) [0.9] (P = 0.15)	0.38 ± 0.05	2.9 ± 1.0 [7.6] (P = 0.0069)	1.1 ± 0.8	0.5 ± 0.4 [0.45] (P = 0.55)
Choline	N.D.*	3.7 ± 0.1 (220) (P = N.D.)	0.015 ± 0.003	0.14 ± 0.008 [9.3] (P < 0.0001)	N.D*	1.7 ± 0.5 (P = N.D.)
Cytisine	5.3 ± 0.5 (4.6)	5.4 ± 0.3 (4.0) [1.0] (P = 0.91)	0.053 ± 0.01	0.53 ± 0.06 [9.9] (P < 0.0001)	0.94 ± 0.98	1.0 ± 0.6 [1.1] (P = 0.95)

N.D., not determined.
* Value could not be accurately determined because of low efficacy of choline.

can provide clues to the mechanism underlying the actions of the modulator. We investigated dFBr's influence on the full agonist ACh and the partial agonists nicotine, choline, and cytisine. ACh and choline were examined to explore possible physiological effects of dFBr within the synapse. Although choline has not previously been considered a partial agonist at α4β2 receptors, the observed effects of dFBr on agonist efficacies led us to consider whether choline might be revealed as an agonist for α4β2 receptors in the presence of dFBr. Nicotine, a common substance of abuse, was selected because of its pathological significance in drug addiction. Cytisine was chosen because it is a α4β2 partial agonist that does not induce channel block (Liu et al., 2008). In addition, the smoking cessation drug varenicline is a derivative of cytisine that allows us to explore dFBr's potential influence on this therapeutic treatment (Coe et al., 2005). dFBr's alterations of response profiles, pEC_{50} (−log EC_{50}), I_{max}, and Hill coefficients (n_H) for full and partial agonists are shown in Figs. 2 and 3 and Table 1, respectively.

Figure 2 shows responses of α4β2 receptors to different concentrations of agonist applied alone (left series of traces) or with increasing concentrations of dFBr at a fixed (EC_{75}) concentration of agonist or partial agonist (right series of traces). Agonist control responses show increases in the rise time and peak responses with increasing agonist concentrations (Fig. 2). The desentization profiles remain unaltered, although this is difficult to determine from responses obtained by using the weak partial agonists choline and cytisine. Coapplication of increasing concentrations of dFBr altered the profile of responses induced by agonists and partial agonists (Fig. 2). As dFBr concentration is increased, responses to ACh, nicotine, choline, and cytisine show marked increases in the rise time of the response and peak currents. Desensitization rates are initially unchanged at low dFBr concentrations but increase as the concentration of dFBr is increased. This increase in the desensitization rate does not seem to occur with cytisine. Changes in responses resulting from application of dFBr were identical whether

dFBr was coapplied or applied before addition of ACh (results not shown).

The apparent pEC_{50}, efficacy, and Hill coefficients (n_H) for each agonist were determined from concentration response data and are shown in Fig. 3 and Table 1. The pEC_{50} values for the tested agonist were not altered by coapplication of 1 μM dFBr. Choline invoked extremely small currents, making determination of pEC_{50} values in the absence of dFBr difficult and making it impossible to determine whether the pEC_{50} changed as a result of dFBr application.

I_{max} values increased significantly in all cases and seemed to increase more substantially for weak partial agonists compared with the stronger partial agonist nicotine and the full agonist ACh (Table 1; Fig. 3). A 2.70-fold increase in the I_{max} was observed for ACh in the presence of 1 μM dFBr ($p < 0.0001$), whereas an increase of more than 9.0-fold was observed for the weak partial agonists choline and cytisine ($p < 0.0001$). Increases in I_{max} for ACh are consistent with previously reported data for ACh (Sala et al., 2005; Kim et al., 2007). I_{max} values obtained for nicotine indicate a nonsignificant increase of 7.6-fold in the presence of 1 μM dFBr ($p = 0.0069$) compared with nicotine alone. The maximum potentiated responses to weak partial agonists failed to reach similar amplitudes to potentiated responses of the full agonist ACh (Table 1). Hill slopes were not significantly altered for any of the four agonists tested.

dFBr Does Not Seem to Alter Inhibition by Antagonists. Because antagonists are typically thought to bind to the closed state of the receptor and do not stabilize the open conformation, they can be used to determine whether application of dFBr produces a conformational change in the orthosteric binding site of the antagonist bound conformation. It is also possible that known antagonists might only weakly stabilize the open state and act as very poor partial agonists (similar to choline). These compounds might reveal themselves as agonists in the presence of modulators such as dFBr. We evaluated the effects of dFBr on three different nAChR antagonists (DHβE, DMAB-anabaseine, and tropisetron). Compounds with diverse actions, selectivity, and structures were chosen. DMAB-anabaseine is a partial agonist on α7 nAChRs but a competitive antagonist on other nAChRs, including the α4β2 subtype (Stevens et al., 1998). DHβE is a neuronal nAChR α4-selective competitive antagonist (Harvey et al., 1996), and tropisetron is a 5-HT$_3$ and α4β2 nAChR receptor competitive antagonist (Middlemiss and Tricklebank, 1992).

Antagonists were evaluated for their ability to inhibit responses to 1 mM ACh on α4β2 nAChR-expressing oocytes in the presence and absence of 1 μM dFBr (Fig. 4). pIC_{50} ($-\log IC_{50}$) values were determined from these data and compared (Fig. 4). No significant change in pIC_{50} was observed for DHβE or tropisetron (Fig. 4). In the presence of dFBr, the DMAB-anabaseine pIC_{50} was increased significantly ($p < 0.0001$). The dose–response curve of coapplication of dFBr and DMAB seems biphasic; however, fitting the data to a two-site model did not produce any improvement compared with the single-site model (single site, $r^2 = 0.77$; two site, $r^2 = 0.77$). It is possible that a biphasic curve could be produced as a result of expression of both high- and low-affinity α4β2 stoichiometries. It has been shown that DHβE has different inhibitory effects on the two different receptor stoichiometries (Moroni et al., 2006). DMAB-

anabaseine may have similar effects, but to our knowledge this ligand has not been tested on high- and low-affinity α4β2 nAChRs.

To determine whether dFBr could stimulate an agonist-like response with antagonists, 1 μM dFBr was coapplied in the absence of ACh at antagonist concentrations up to 100 μM. No currents were observed under these conditions.

dFBr Can Reactivate Desensitized Receptors. To examine the effect of dFBr on desensitized receptors, dFBr was applied to α4β2 receptors desensitized with saturating concentrations of ACh (Fig. 5). In the absence of dFBr repeated application of 10 mM ACh during the desensitization period of the response elicits no additional current (Fig. 5A, top). This is consistent with the presence of a large number of desensitized receptors in the preparation that are resistant to reactivation by ACh. Application of 3-s pulses of dFBr applied during the desensitized phase produced large inward currents (Fig. 5A, bottom). Repeated 3-s applications of dFBr produced a series of responses with progressively decreasing peak currents (Fig. 5, B and C). When responses were elicited using 1 mM ACh (Fig. 5B), rather than 10 mM ACh, activation with 1 μM dFBr produced hump currents immediately after the 3-s dFBr pulse. The activation slope for the first dFBr pulse obtained during the desensitization period was -190 ± 9 nA/s for 1 mM ACh-induced responses and -1020 ± 130 nA/s for 10 mM ACh-induced responses. Activation slopes for responses in which dFBr and ACh were coapplied to nondesensitized receptors as shown in Fig. 2 were also determined: 1 mM ACh + 1 μM dFBr, -13 ± 2 nA/s and 10 mM ACh + 1 μM dFBr, -66 ± 6 nA/s. Thus, the activation slope of the response to a dFBr pulse applied during desensitization is 15 times faster than coapplication of ACh and dFBr to nondesensitized receptors. This is a significant change in the activation slope ($p < 0.001$). When 100 μM cytisine was used as the stimulating agonist and dFBr was applied during the desensitizing phase, a similar effect was observed (Fig. 5C). Repeated 3-s applications of 1 μM dFBr along with continuous application of 100 μM cytisine produced repeated responses that decline only slightly in amplitude with each repetition. The activation slope for the first dFBr pulse applied during the desensitization phase of responses to 100 μM cytisine was -66 ± 26 nA/s compared with -0.66 ± 0.18 nA/s for coapplication of 1 μM dFBr and 100 μM cytisine to nondesensitized receptors. This is a significant increase ($p < 0.01$) in the activation slope of approximately 100-fold.

dFBr-Induced Currents Elicited on Desensitized Receptors Decline with Continuous Exposure to dFBr. The data shown in Fig. 5 demonstrate the effect of a quick pulse of dFBr applied during the desensitization phase of the response. It was unclear from these experiments whether dFBr-elicited responses on desensitized receptors would show typical desensitizing kinetics during longer exposures to dFBr. To determine whether receptors desensitize in the continued presence of dFBr, we conducted experiments in which desensitized nAChR preparations were exposed to dFBr for longer time periods. Figure 6 shows the effects of application of 1 μM dFBr for 48 s to receptors pre-exposed to ACh. Coexposure of oocytes to 1 mM ACh and 1 μM dFBr for 48 s produces a typical dFBr-potentiated response (Fig. 6A). As in Fig. 5A, bath application of a control pulse of 1 mM ACh for 48 s after the response peak produces no additional cur-
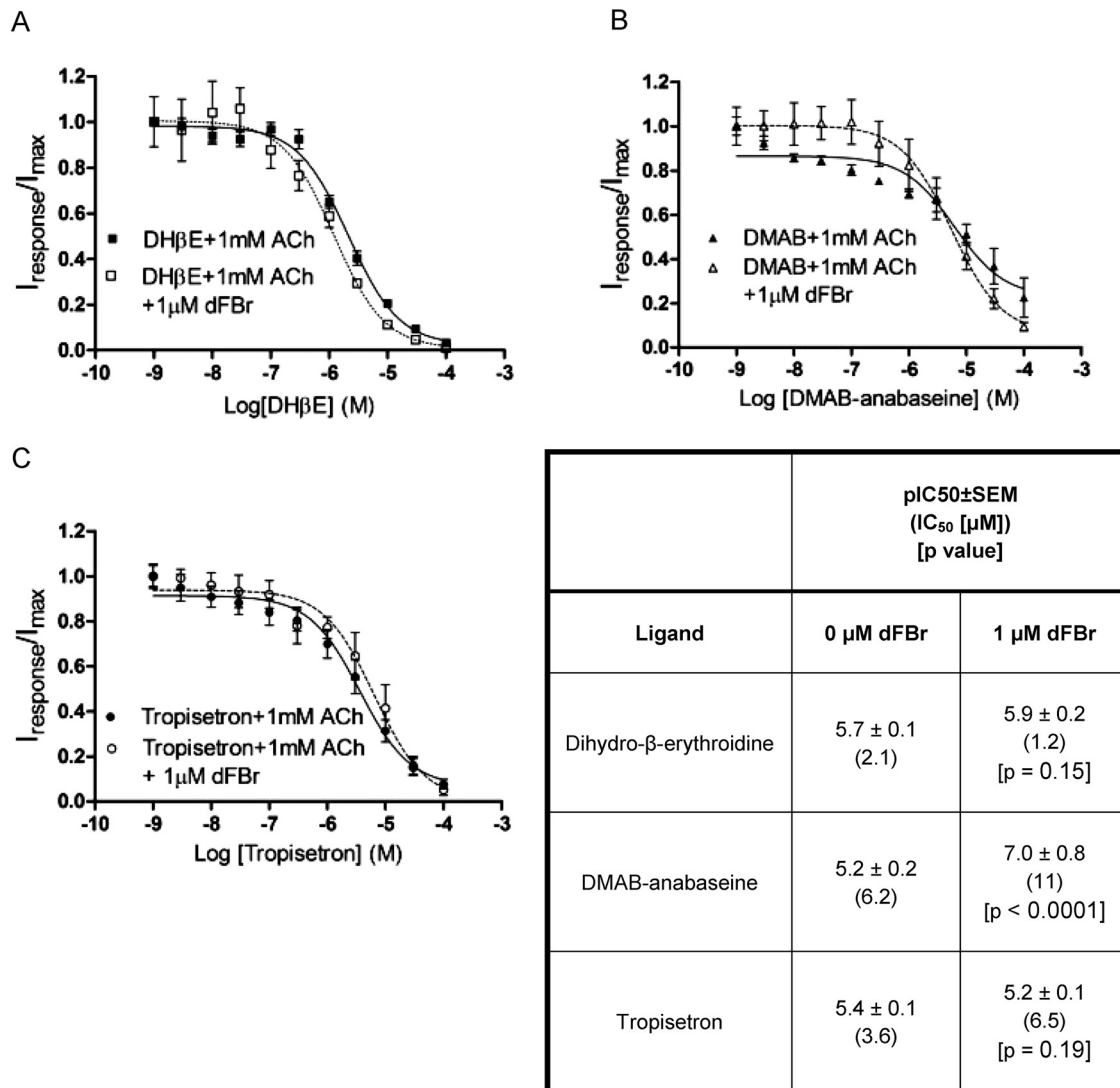
A

B

C

Ligand	pIC50±SEM (IC$_{50}$ [μM]) [p value]	
	0 μM dFBr	1 μM dFBr
Dihydro-β-erythroidine	5.7 ± 0.1 (2.1)	5.9 ± 0.2 (1.2) [p = 0.15]
DMAB-anabaseine	5.2 ± 0.2 (6.2)	7.0 ± 0.8 (11) [p < 0.0001]
Tropisetron	5.4 ± 0.1 (3.6)	5.2 ± 0.1 (6.5) [p = 0.19]

Fig. 4. Coapplication of dFBr with nAChR antagonists. *Xenopus* oocytes expressing α4β2 receptors (mRNA injected at a ratio of 1α/1β) were exposed to 1 mM ACh, and responses were inhibited by coapplication of increasing concentrations of DHβE (A), DMAB-anabaseine (B), or troposetron (C). Because individual peak amplitudes were normalized to those elicited by 1 mM ACh applied alone on the same oocyte, I_{max} values express peak currents relative to those obtained with 1 mM ACh. pIC$_{50}$ values (bottom right) were determined by using nonlinear curve fitting as described under *Materials and Methods*. Data points represent at least four replicate values obtained from a minimum of two oocytes harvested from different frogs. Error bars indicate ± S.E.M.

rent (Fig. 6B). Application of 1 μM dFBr for 48 s immediately after the ACh response peak and in the continued presence of 1 mM ACh (Fig. 6C) produces a response similar in shape and amplitude to that resulting from coexposure to ACh and dFBr (Fig. 6A). A similar experiment in which 1 μM dFBr was applied concurrent with termination of the ACh perfusion produced a different response (Fig. 6D). When 1 mM ACh was replaced rapidly by 1 μM dFBr after the response peak, a more rapidly desensitizing and sharper response peak was observed. When 1 μM dFBr was again replaced with 1 mM ACh a similar sharp peak was observed, although with an apparently slower rate of desensitization. In all cases, where 1 μM dFBr was applied, either in conjunction with 1 mM ACh or after the 1 mM ACh peak (Fig. 6, A, C, and D), removal of dFBr returned the response to its appropriate nonpotentiated level. Thus, application of 1 μM dFBr produces peak responses that appear superimposed on the 1 mM ACh response.

Discussion

Previous studies demonstrate that the potentiating effects of dFBr and its apparent selectivity (based on previous studies) for the α4β2 subtype of nAChRs make it an ideal candidate for the development of novel PAMS for α4β2 nAChRs (Sala et al., 2005; Kim et al., 2007). The work described here addresses three elements of dFBr modulation on α4β2 nAChR important to its ultimate development as a therapeutic agent: 1) the nature of its bell-shaped response profile; 2) its effect on the action of α4β2 nicotinic full agonists, partial agonists, and antagonists; and 3) its effect on receptor kinetics.

The Bell-Shaped Dose Response of dFBr. We have previously demonstrated the ability of synthetic dFBr to potentiate ACh-induced responses at concentrations less than 10 μM and inhibit responses at concentrations higher than 10 μM dFBr (Kim et al., 2007). The observation of
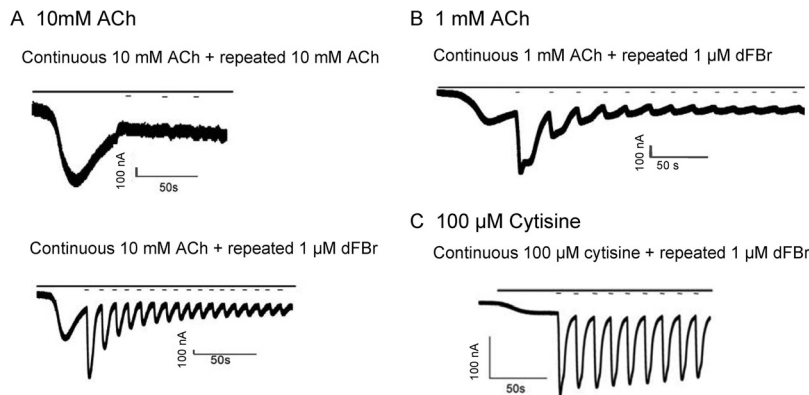
Fig. 5. dFBr reactivates desensitized receptors. Acetylcholine or cytisine were bath-applied to *Xenopus* oocytes expressing α4β2 receptors at a rate of 3 ml/min for 30 s. During the desensitized portion of the response, 3-s pulses of either acetylcholine (A, top) or dFBr (A, bottom, B, and C) were repeatedly applied at a perfusion rate of 20 ml/min in the continued presence of agonist. Solid bars above the traces show the application of ACh or cytisine (continuous bar) and the repeated pulsed application of 1 μM dFBr (short lines on A, bottom, B, and C plots). A top, control trace showing repeated pulses of 10 mM acetylcholine applied during the desensitization period of a response to bath-applied 10 mM ACh. Minimal current was observed under these conditions. A bottom, application of 3-s pulses of 1 μM dFBr during the desensitization period produces large currents that decline back to baseline with repeated pulses of dFBr. B, application of 3-s pulses of 1 μM dFBr during the desensitization period of responses to 1 mM ACh produces similar effects to A bottom except pulses are broadened and show possible hump currents. C, application of 3-s pulses of 1 μM dFBr during the desensitization period of responses to 100 μM cytisine. Large currents were observed similar to those shown in A bottom but with a slower rate of decline. Each experiment was repeated at least four times on different oocytes harvested from at least two different frogs. The slope of the rising phase of the first peak generated by application of dFBr during the desensitizing period in each case was determined (activation slope): A bottom, -1020 ± 130 nA/s; B, -190 ± 9 nA/s; C, -66 ± 26 nA/s.
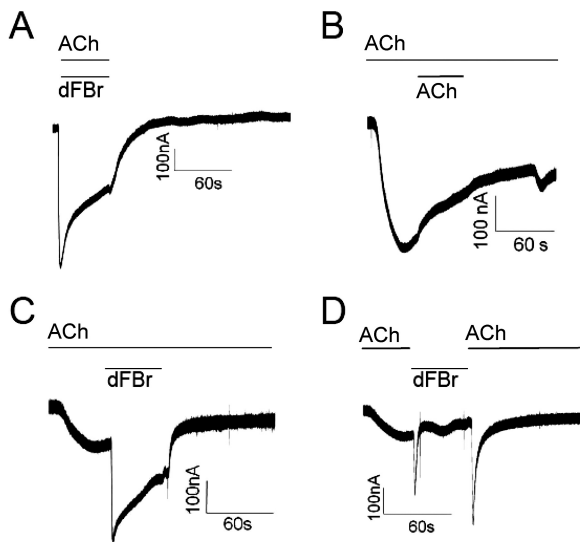

Fig. 6. The amplitudes of dFBr-induced currents on desensitized receptors decline during long exposures to dFBr. Responses were elicited by bath application of 1 mM ACh on *Xenopus* oocytes expressing α4β2 receptors. The top solid line above each trace indicates the time period during which the oocyte was exposed to ACh. The bottom line above the trace indicates the period of application of either ACh or dFBr (A, C, and D). A, coapplication of 1 mM ACh and 1 μM dFBr for 48 s at a flow rate of 8 ml/min (no pre-exposure to ACh). B, control trace resulting from exposure to 1 mM ACh at a rate of 4 ml/min with 1 mM ACh applied during the desensitization period for 48 s at 8 ml/min. C, application of 1 μM dFBr at the peak of a response elicited by exposure to 1 mM ACh. ACh was present before, during, and after application of dFBr. D, application of 1 μM dFBr at the peak of a response elicited by exposure to 1 mM ACh. Unlike the experiment shown in C, perfusion of 1 mM ACh was discontinued during the application of 1 mM dFBr then restored at the end of the 48-s dFBr exposure. The responses shown were obtained from different oocytes. Because of different levels of receptor expression, no comparison of peak amplitudes was possible under these conditions.

rebound currents on washout of dFBr/agonist led us to hypothesize that dFBr produced inhibition of ACh responses though a mechanism involving open-channel block (Kim et al., 2007; Liu et al., 2008). The nonlinear *V/I* relationship of

dFBr inhibition observed in voltage step experiments strongly supports our hypothesis that dFBr inhibition results from open-channel block.

ACh has been previously demonstrated to inhibit its own responses by blocking the ion channel at high concentrations. To determine whether dFBr could also block the channel, we conducted experiments with the nonchannel blocking partial agonist cytisine as the stimulating agonist (Liu et al., 2008). The nonlinear *V/I* relationship at dFBr concentrations >10 μM suggests that dFBr itself is capable of channel block. The linear *V/I* relationship at dFBr concentrations <10 μM supports our hypothesis that potentiation and inhibition are mediated by different mechanisms. This suggests that future analogs of dFBr could be developed that do not inhibit α4β2 nAChRs and are better able to potentiate agonist responses with less effect on the apparent desensitization kinetics.

The Effect of dFBr on the Action of Nicotinic Agonists and Partial Agonists. We examined the ability of dFBr to enhance the action of other compounds involved in nAChR signaling including choline, nicotine, and cytisine. Both nicotine and verenecline (a derivative of cytisine) are being explored and/or used as therapeutic agents. dFBr did not alter the pEC_{50} of ACh, choline, nicotine, and cytisine. I_{max} values for all three partial agonists were increased with a much more substantial enhancement obtained for the low-efficacy partial agonists choline (9.3×) or cytisine (9.9×) than for the higher-efficacy agonist nicotine (7.6×). dFBr coapplied with choline produced a response of approximately 12% of the nonpotentiated ACh response. Although it is difficult to extrapolate the effects on synaptic function from receptors expressed in *Xenopus* oocytes, it is likely that increased activation by choline would alter the time course for synaptic currents. The nicotine response during dFBr coapplication was equivalent to a nonpotentiated response to ACh. This raises the possibility of future therapies combining a lower nicotine dose with a dFBr class compound.

dFBr coapplication did not alter the pEC_{50} values for ACh, nicotine, or cytisine. These observations, along with the en-

hanced affinity for the antagonist DMAB-anabaseine, lead us to conclude that dFBr may alter relative stabilities of receptor conformations involved in channel gating (channel opening and desensitization).

The Effect of dFBr on Inhibition of Responses by Nicotinic Antagonists. We evaluated the ability of three structurally different competitive antagonists (DHβE, DMAB-anabaseine, and tropisetron) to inhibit responses to ACh in the presence and absence of dFBr. No significant changes in inhibition kinetics were observed for DHβE and tropisetron. DMAB-anabaseine, a α7 partial agonist, produced a 1.4-fold increase in its pIC_{50} value with the application of 1 μM dFBr. The effect of dFBr on antagonist pIC_{50} values seems to be minimal.

Conformational changes induced by allosteric modulators could alter the orthosteric binding site, causing an antagonist (or poor agonist) to become a functional agonist. The benzodiazepine flurazepam induces conformational rearrangements in the GABA binding site on GABA type A receptor, demonstrating shared allosteric interactions between the GABA and benzodiazepine binding sites (Kloda and Czajkowski, 2007). To determine whether a similar action might occur with nicotinic antagonists, we examined the effects of dFBr coapplication with antagonists in the absence of stimulating ACh. We did not observe any currents for any antagonist tested, including the α7 partial agonist DMAB-anabaseine. The lack of any change in antagonist action suggests that dFBr does not produce its effects through alteration of the unbound, closed receptor conformation. This further supports our hypothesis that dFBr potentiation is the result of alterations in gating rather than ligand binding.

Recovery of Desensitized Receptors by dFBr. Several possible mechanisms could produce the observed changes in partial agonist apparent efficacies. Agonist efficacy has been correlated to varying degrees of C-loop closure over the ligand seated within the orthosteric binding pocket in ionotropic glutamate receptor, glycine receptors, and ACh binding protein (Armstrong and Gouaux, 2000; Hogner et al., 2002; Armstrong et al., 2003; Furukawa and Gouaux, 2003; Jin et al., 2003; Celie et al., 2004; Han et al., 2004; Hansen et al., 2005). Further studies suggest that efficacy of agonists at both ionotropic glutamate and glycine receptors are determined by the ability of the agonist to stabilize the active receptor conformation (Furukawa and Gouaux, 2003; Han et al., 2004; Inanobe et al., 2005; Robert et al., 2005; Mayer, 2006). In a model for glycine and nAChRs agonist efficacy differences are suggested to originate in the agonist affinity for a hypothesized flipped state relative to the closed state (Lape et al., 2008). Stabilization of the open conformation could also shift the equilibrium from the desensitized to the open state. One implication of the latter mechanism would be the possibility that application of dFBr to a desensitized receptor population would elicit currents by reactivating desensitized receptors. This ability has previously been reported for type II PAMs including PNU-120596 [1-(5-chloro-2,4-dimethoxyphenyl)-3-(5-methylisoxazol-3-yl)urea] and TQS [4-aphthalene-1-yl-3*a*,4,5,9*b*-tetrahydro-3-*H*-cyclopenta[*c*]quinoline-8-sulfonic acid] (Hurst et al., 2005; Bertrand and Gopalakrishnan, 2007; Grønlien et al., 2007) but not for dFBr.

To determine whether dFBr could reactivate desensitized receptors dFBr was applied during the desensitization period of a 1 mM ACh-elicited response. Large currents were observed in response to dFBr application that were similar in magnitude to those obtained for a control exposure of ACh to nondesensitized receptors. These responses decline rapidly on removal of dFBr. With longer exposures responses desensitized in the continuous presence of dFBr and ACh, returning to the pre-dFBr level on removal of the modulator. The decline in the dFBr-elicited response over time could be the result of open channel block by both ACh and dFBr as described earlier but could also reflect the existence of a desensitized open conformation that relaxes to a new desensitized state in the continued presence of dFBr as has been proposed for ivermectin (Krause et al., 1998; Grønlien et al., 2007). The observed decline in the response is similar to that observed when dFBr is coapplied with ACh to nondesensitized receptors, but the time to peak is significantly shortened. This would be consistent with either independent binding of ACh and dFBr or a requirement for ACh to bind first.

When dFBr is applied to desensitized receptors with the simultaneous removal of ACh, a large peak is elicited that quickly returns to the pre-dFBr amplitude. A second switch from perfusion with dFBr back to ACh produces an ACh-elicited peak in the absence of dFBr that also desensitizes rapidly back to the baseline response amplitude. These data suggest that ACh and dFBr bind independently with no requirement for ACh to bind before dFBr or vice versa. The rapid rise of the response peaks in Fig. 6D seems to be the result of either ACh bound first followed by dFBr (first peak) or dFBr bound followed by ACh activation (second peak). The rapid decline of the first peak (Fig. 6D) is probably the result of ACh dissociation from the receptor during dFBr application, and the decline of the second peak represents dissociation of dFBr from the receptor. Thus the rate of decline in Fig. 6D may be reflective of the dissociation rates for either ACh (left trace) or dFBr (right peak).

It has been postulated that the ability to reopen desensitized receptors could be a common feature of type II modulators (Galzi et al., 1992; Briggs et al., 1999). Thus, dFBr could be classified as a α4β2 type II PAM. Some concern has been expressed regarding alterations in desensitization rates by type II PAMs because such changes might adversely affect cell viability caused by increased Ca^{2+} permeability. This remains a concern with dFBr, particularly because of its ability to reopen desensitized receptors. The balance between potentiation and channel block may be an important consideration therapeutically because channel block could reduce the problem of Ca^{2+} entry through the channel. The combined channel block and potentiation with dFBr produces sharper, more rapidly desensitizing responses rather then prolonged openings as have been observed in type II PAMs. The enhancement of partial agonist activities presents the possibility for combination therapies between dFBr-like compounds and therapeutic partial agonists.

References

Adams CE and Stevens KE (2007) Evidence for a role of nicotinic acetylcholine receptors in schizophrenia. *Front Biosci* **12:**4755–4772.
Armstrong N and Gouaux E (2000) Mechanisms for activation and antagonism of an AMPA-sensitive glutamate receptor: crystal structures of the GluR2 ligand binding core. *Neuron* **28:**165–181.

Armstrong N, Mayer M, and Gouaux E (2003) Tuning activation of the AMPA-sensitive GluR2 ion channel by genetic adjustment of agonist-induced conformational changes. *Proc Natl Acad Sci USA* **100:**5736–5741.

Aubert I, Araujo DM, Cécyre D, Robitaille Y, Gauthier S, and Quirion R (1992) Comparative alterations of nicotinic and muscarinic binding sites in Alzheimer's and Parkinson's diseases. *J Neurochem* **58:**529–541.

Bertrand D and Gopalakrishnan M (2007) Allosteric modulation of nicotinic acetylcholine receptors. *Biochem Pharmacol* **74:**1155–1163.

Bourin M, Ripoll N, and Dailly E (2003) Nicotinic receptors and Alzheimer's disease. *Curr Med Res Opin* **19:**169–177.

Briggs CA, McKenna DG, Monteggia LM, Touma E, Roch JM, Arneric SP, Gopalakrishnan M, and Sullivan JP (1999) Gain of function mutation of the α7 nicotinic receptor: distinct pharmacology of the human α7V274T variant. *Eur J Pharmacol* **366:**301–308.

Celie PH, van Rossum-Fikkert SE, van Dijk WJ, Brejc K, Smit AB, and Sixma TK (2004) Nicotine and carbamylcholine binding to nicotinic acetylcholine receptors as studied in AChBP crystal structures. *Neuron* **41:**907–914.

Coe JW, Brooks PR, Vetelino MG, Wirtz MC, Arnold EP, Huang J, Sands SB, Davis TI, Lebel LA, Fox CB, et al. (2005) Varenicline: an α4β2 nicotinic receptor partial agonist for smoking cessation. *J Med Chem* **48:**3474–3477.

Corey-Bloom J (2003) Galantamine: a review of its use in Alzheimer's disease and vascular dementia. *Int J Clin Pract* **57:**219–223.

Court J, Martin-Ruiz C, Piggott M, Spurden D, Griffiths M, and Perry E (2001) Nicotinic receptor abnormalities in Alzheimer's disease. *Biol Psychiatry* **49:**175–184.

Friedman JI (2004) Cholinergic targets for cognitive enhancement in schizophrenia: focus on cholinesterase inhibitors and muscarinic agonists. *Psychopharmacology (Berl)* **174:**45–53.

Furukawa H and Gouaux E (2003) Mechanisms of activation, inhibition and specificity: crystal structures of the NMDA receptor NR1 ligand-binding core. *EMBO J* **22:**2873–2885.

Galzi JL, Devillers-Thiéry A, Hussy N, Bertrand S, Changeux JP, and Bertrand D (1992) Mutations in the channel domain of a neuronal nicotinic receptor convert ion selectivity from cationic to anionic. *Nature* **359:**500–505.

Grønlien JH, Håkerud M, Ween H, Thorin-Hagene K, Briggs CA, Gopalakrishnan M, and Malysz J (2007) Distinct profiles of α7 nAChR positive allosteric modulation revealed by structurally diverse chemotypes. *Mol Pharmacol* **72:**715–724.

Han NL, Clements JD, and Lynch JW (2004) Comparison of taurine- and glycine-induced conformational changes in the M2–M3 domain of the glycine receptor. *J Biol Chem* **279:**19559–19565.

Hansen SB, Sulzenbacher G, Huxford T, Marchot P, Taylor P, and Bourne Y (2005) Structures of Aplysia AChBP complexes with nicotinic agonists and antagonists reveal distinctive binding interfaces and conformations. *EMBO J* **24:**3635–3646.

Harvey SC, Maddox FN, and Luetje CW (1996) Multiple determinants of dihydro-β-erythroidine sensitivity on rat neuronal nicotinic receptor α subunits. *J Neurochem* **67:**1953–1959.

Hogner A, Kastrup JS, Jin R, Liljefors T, Mayer ML, Egebjerg J, Larsen IK, and Gouaux E (2002) Structural basis for AMPA receptor activation and ligand selectivity: crystal structures of five agonist complexes with the GluR2 ligand-binding core. *J Mol Biol* **322:**93–109.

Hurst RS, Hajós M, Raggenbass M, Wall TM, Higdon NR, Lawson JA, Rutherford-Root KL, Berkenpas MB, Hoffmann WE, Piotrowski DW, et al. (2005) A novel positive allosteric modulator of the α7 neuronal nicotinic acetylcholine receptor: in vitro and in vivo characterization. *J Neurosci* **25:**4396–4405.

Inanobe A, Furukawa H, and Gouaux E (2005) Mechanism of partial agonist action at the NR1 subunit of NMDA receptors. *Neuron* **47:**71–84.

Jin R, Banke TG, Mayer ML, Traynelis SF, and Gouaux E (2003) Structural basis for partial agonist action at ionotropic glutamate receptors. *Nat Neurosci* **6:**803–810.

Joshi PR, Suryanarayanan A, and Schulte MK (2004) A vertical flow chamber for *Xenopus* oocyte electrophysiology and automated drug screening. *J Neurosci Methods* **132:**69–79.

Kim JS, Padnya A, Weltzin M, Edmonds BW, Schulte MK, and Glennon RA (2007) Synthesis of desformylflustrabromine and its evaluation as an α4β2 and α7 nACh receptor modulator. *Bioorg Med Chem Lett* **17:**4855–4860.

Kloda JH and Czajkowski C (2007) Agonist-, antagonist-, and benzodiazepine-induced structural changes in the α1 Met113–Leu132 region of the GABAA receptor. *Mol Pharmacol* **71:**483–493.

Krause RM, Buisson B, Bertrand S, Corringer PJ, Galzi JL, Changeux JP, and Bertrand D (1998) Ivermectin: a positive allosteric effector of the α7 neuronal nicotinic acetylcholine receptor. *Mol Pharmacol* **53:**283–294.

Lape R, Colquhoun D, and Sivilotti LG (2008) On the nature of partial agonism in the nicotinic receptor superfamily. *Nature* **454:**722–727.

Lippiello PM (2006) Nicotinic cholinergic antagonists: a novel approach for the treatment of autism. *Med Hypotheses* **66:**985–990.

Liu Q, Yu KW, Chang YC, Lukas RJ, and Wu J (2008) Agonist-induced hump current production in heterologously-expressed human α4β2-nicotinic acetylcholine receptors. *Acta Pharmacol Sin* **29:**305–319.

Martin-Ruiz CM, Lee M, Perry RH, Baumann M, Court JA, and Perry EK (2004) Molecular analysis of nicotinic receptor expression in autism. *Brain Res Mol Brain Res* **123:**81–90.

Mayer ML (2006) Glutamate receptors at atomic resolution. *Nature* **440:**456–462.

Middlemiss DN and Tricklebank MD (1992) Centrally active 5-HT receptor agonists and antagonists. *Neurosci Biobehav Rev* **16:**75–82.

Moroni M, Zwart R, Sher E, Cassels BK, and Bermudez I (2006) α4β2 nicotinic receptors with high and low acetylcholine sensitivity: pharmacology, stoichiometry, and sensitivity to long-term exposure to nicotine. *Mol Pharmacol* **70:**755–768.

Nicolson R, Craven-Thuss B, and Smith J (2006) A prospective, open-label trial of galantamine in autistic disorder. *J Child Adolesc Psychopharmacol* **16:**621–629.

Nordberg A (2001) Nicotinic receptor abnormalities of Alzheimer's disease: therapeutic implications. *Biol Psychiatry* **49:**200–210.

Robert A, Armstrong N, Gouaux JE, and Howe JR (2005) AMPA receptor binding cleft mutations that alter affinity, efficacy, and recovery from desensitization. *J Neurosci* **25:**3752–3762.

Sala F, Mulet J, Reddy KP, Bernal JA, Wikman P, Valor LM, Peters L, König GM, Criado M, and Sala S (2005) Potentiation of human α4β2 neuronal nicotinic receptors by a *Flustra foliacea* metabolite. *Neurosci Lett* **373:**144–149.

Stevens KE, Kem WR, Mahnir VM, and Freedman R (1998) Selective α7-nicotinic agonists normalize inhibition of auditory response in DBA mice. *Psychopharmacology (Berl)* **136:**320–327.

Woodruff-Pak DS and Gould TJ (2002) Neuronal nicotinic acetylcholine receptors: involvement in Alzheimer's disease and schizophrenia. *Behav Cogn Neurosci Rev* **1:**5–20.

Address correspondence to: Marvin K. Schulte, Department of Chemistry and Biochemistry, University of Alaska, 900 Yukon Drive, Fairbanks, AK 99775. E-mail: mkschulte@alaska.edu